



## Measurements of atmospheric ethene by solar absorption FTIR spectrometry

Geoffrey C. Toon, Jean-Francois L. Blavier, Keeyoon Sung  
Jet Propulsion Laboratory, California Institute of Technology, CA 91109, USA

5 *Correspondence to:* [Geoffrey.C.Toon@jpl.nasa.gov](mailto:Geoffrey.C.Toon@jpl.nasa.gov)

**Abstract.** Atmospheric ethene ( $C_2H_4$ ; ethylene) amounts have been retrieved from high-resolution solar absorption spectra measured by the JPL MkIV interferometer. Data recorded from 1985 to 2016 from a dozen ground-based sites have been analyzed. At clean-air sites such as Alaska, Sweden, New Mexico, or the mountains of California, the ethene column was always  
10 less than  $10^{15}$  molec. $cm^{-2}$  and therefore undetectable. In urban sites such as Pasadena, California, ethane was measurable with column amounts of  $20 \times 10^{15}$  molec. $cm^{-2}$  observed in the 1990's. Despite the increasing population and traffic in Southern California, a factor 3 decrease in ethene column density is observed over Pasadena in the past 25 years, accompanied by a decrease in  $CO_2$ . This is likely due to Southern California's increasingly stringent vehicle exhaust regulations and  
15 tighter enforcement over this period.

### Introduction

Atmospheric ethene is formed primarily by incomplete combustion. This can be due to biomass burning, power plants, combustion engines, etc. There are still large uncertainties in ethene emissions. Sawada and Totsuka (1986) used measurements of ethene emissions per unit  
20 biomass to derive a global source of 17 - 29 Tg  $yr^{-1}$ . Goldstein et al. (1996) measured ethene emissions from Harvard forest (MA), and found that they were linearly correlated with levels of PAR, indicating a photosynthetic source. Using these fluxes, and the ecosystem areas tabulated by Sawada and Totsuka (1986), global biogenic sources for ethene of 21 Tg  $yr^{-1}$  respectively were calculated. This value is similar to the estimates of Hough (1991) and Table 3 of Sawada and  
25 Totsuka (1986). The ethene fluxes listed by Poisson et al. (2000), however, are only 11.8 Tg  $yr^{-1}$ , while those of Muller and Brasseur [1995] are only 5 Tg  $yr^{-1}$ . Combustion of fossil fuels amounts to only 21% of global anthropogenic emissions, but in urban areas this can be the major source. Ethene is primarily destroyed by reaction with OH (Olivella and Sole, 2004), which is rapid, giving ethene a tropospheric lifetime of only 1 to 3 days.

30 There have been previous measurements of ethene by in situ techniques and also by remote sensing. These will be discussed later in the context of comparisons with MkIV results.



We report here long-term remote sensing measurements of  $C_2H_4$  in the lower troposphere, where the vast majority of  $C_2H_4$  resides, by ground-based MkIV observations. We also present MkIV balloon measurements of  $C_2H_4$  in the upper troposphere.

### 35 MkIV instrument

The MkIV FTS is a double-passed FTIR spectrometer designed and built at JPL in 1984 for atmospheric observations [Toon, 1991]. It covers the entire  $650\text{--}5650\text{ cm}^{-1}$  region simultaneously with two detectors: a HgCdTe photoconductor covering  $650\text{--}1800\text{ cm}^{-1}$  and an InSb photodiode covering  $1800\text{--}5650\text{ cm}^{-1}$ . The MkIV instrument has flown 23 balloon flights since 1989. It has also flown on over 40 flights of the NASA DC-8 aircraft as part of various campaigns during 1987 to 1992 studying high-latitude ozone loss. MkIV has also made 1090 days of ground-based observations since 1985 from a dozen different sites, from Antarctica to the Arctic, from sea-level to 3.8 km altitude. Details of the ground-based measurements and sites can be found at: <http://mark4sun.jpl.nasa.gov/ground.html>. MkIV observations have been extensively compared with satellite remote sounders (e.g. Velazco et al. 2009) and with in situ data (e.g., Toon et al., 1999a,b).

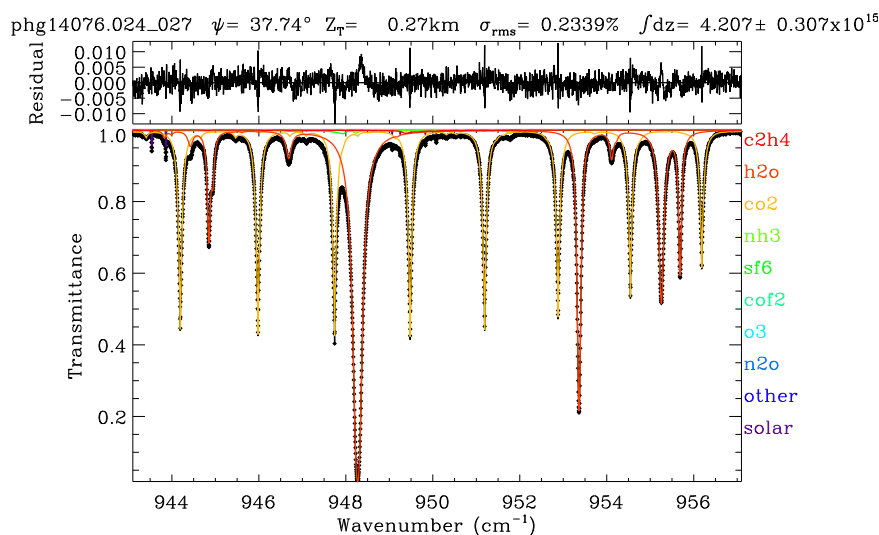


**Figure 1.** Example of a fit to a ground-based MkIV spectrum measured from JPL, California, in March 2014. In the lower panel the black diamond symbols represent the measured spectrum, the black line represents the fitted calculation, and the colored lines represent the contributions of the various absorbing gases; mainly  $CO_2$  (orange) and  $H_2O$  (red). Also fitted are the continuum level, tilt and curvature, a frequency shift, and a solar shift, together with 5 more



55 *weakly absorbing gases ( $\text{NH}_3$ ,  $\text{SF}_6$ ,  $\text{COF}_2$ ,  $\text{O}_3$  and  $\text{N}_2\text{O}$ ). The retrieved  $\text{C}_2\text{H}_4$  column amount on this day,  $4.2 \times 10^{15}$  molec. $\text{cm}^{-2}$ , would represent 2 ppb confined to the lowest 100 mbar (1.5 km) of the atmosphere. The  $\text{C}_2\text{H}_4$  absorption contribution (red) peaks at  $949.35 \text{ cm}^{-1}$  and is less than 1% deep and therefore difficult to discern on this plot. The upper panel shows fitting residuals (measured-calculated), which peak at 1.2% with an rms deviation of 0.235%, are mainly correlated with  $\text{H}_2\text{O}$  and  $\text{CO}_2$ .*

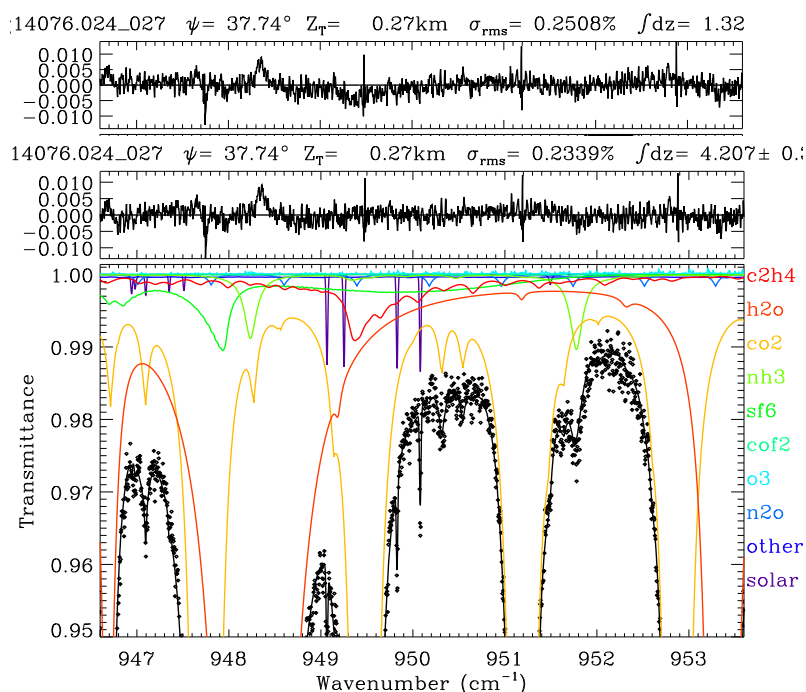
### Analysis Methods

60 The spectral fitting was performed with the GFIT (Gas Fitting) code, a non-linear least-squares algorithm developed at JPL that scales the atmospheric gas volume mixing ratio (vmr) profiles to fit calculated spectra to those measured. For balloon observations, the atmosphere was discretized into 100 layers of 1 km thickness. For ground-based observations, 70 layers of 1 km thickness were used. Absorption coefficients were computed line-by-line assuming a Voigt  
65 lineshape and using the ATM linelist [Toon, 2014a] for the telluric lines. This is a "greatest hits" compilation, founded on HITRAN, but not always the latest version for every band of every gas. In situations where the latest HITRAN version ([Rothman et al., 2012] gave poorer fits, the earlier HITRAN version was retained. The  $\text{C}_2\text{H}_4$  linelist covering the  $950 \text{ cm}^{-1}$  region, containing the  $\nu_7$  and  $\nu_8$  bands, is that described by Rothman et al. [2003]. The solar linelist [Toon, 2014b]  
70 used in the analysis of the ground-based MkIV spectra was obtained from balloon flights of the MkIV instrument.

Sen et al. [1996] provide a more detailed description of the use of the GFIT code for retrieval of vmr profiles from MkIV balloon spectra. GFIT was previously used for the Version 3 analysis [Irion et al., 2003] of spectra measured by the Atmospheric Trace Molecule Occultation  
75 Spectrometer (ATMOS), and is currently used for analysis of TCCON spectra [Wunch et al., 2011] and MKIV spectra [Toon, 2016].

The strongest infrared absorption feature of ethene is the Q-branch of the  $\nu_7$  band ( $\text{CH}_2$  wag) at  $948 \text{ cm}^{-1}$ . This is 7 times stronger than any other feature, including the  $3000 \text{ cm}^{-1}$  region containing the CH-stretch vibrational modes.

80



85

**Figure 2.** Lower and middle panels are as described in Figure 1, but zoomed in to reveal more detail of the  $C_2H_4$  Q-branch (red) at  $949.35\text{ cm}^{-1}$ . Top panel shows residuals from fit performed omitting  $C_2H_4$ . This causes a discernable 0.5% dip in the residuals around  $949.35\text{ cm}^{-1}$  and an increase in the overall rms from 0.234% to 0.251%. The 0.5% dip in the residuals is weaker than the 0.9% depth of the  $C_2H_4$  feature in the upper panel, because the other gases have adjusted to compensate for the omitted  $C_2H_4$ . Their inability to completely do so supports the attribution to  $C_2H_4$ .

90

### Ground-based MkIV Results

Figure 1a shows a fit to the  $943\text{--}957\text{ cm}^{-1}$  region of a ground-based MkIV spectrum measured from JPL, Pasadena. The strongest absorptions are from  $H_2O$  lines (red), one of which is blacked out at  $948.25\text{ cm}^{-1}$ . There are also eight  $CO_2$  lines (orange) in this window with depths of 40–60%, one of which sits directly atop the  $C_2H_4$  Q-branch at  $949.35\text{ cm}^{-1}$ . These  $CO_2$  lines are temperature sensitive, having ground-state energies in the range  $1400 < E < 1600\text{ cm}^{-1}$ . It is not possible to clearly see the  $C_2H_4$  absorption in Fig. 1, and so Fig. 2 zooms into the Q-branch region. The lower panel reveals that the peak  $C_2H_4$  absorption is less than 1% deep and strongly overlapped by  $CO_2$ . It is also overlapped by absorption from  $H_2O$ ,  $SF_6$ ,  $NH_3$ ,  $N_2O$ , and solar OH

100



lines.  $\text{NH}_3$  absorption lines exceed 1% in this window on this particular day but do not overlap the strongest part of the  $\text{C}_2\text{H}_4$  Q-branch. The  $\text{SF}_6$   $\nu_3$  Q-branch at  $947.9\text{ cm}^{-1}$  also exceeds 1% but fortunately does not overlap the  $\text{C}_2\text{H}_4$  Q-branch. The  $\text{SF}_6$  R-branch, however, underlies the  $\text{C}_2\text{H}_4$  Q-branch with about 0.3% absorption depth. The lower panel shows the same spectrum fitted without any  $\text{C}_2\text{H}_4$  absorption. This causes a  $\sim 0.5\%$  dip in the residuals around  $949.35\text{ cm}^{-1}$  and an increase in the overall rms from 0.245 to 0.260%. The 0.5% dip in the residuals is weaker than the 0.9% depth of the  $\text{C}_2\text{H}_4$  feature in the upper panel because the other fitted gases have adjusted to try to compensate for the missing  $\text{C}_2\text{H}_4$ . Their inability to completely do so supports the attribution to  $\text{C}_2\text{H}_4$ .

Given the severity of the interference, especially the directly-overlying 60%-deep  $\text{CO}_2$  line, we were at first skeptical that  $\text{C}_2\text{H}_4$  could be retrieved to a worthwhile accuracy from this window, or any other. But given the good quality of the spectral fits, we nevertheless went ahead and analyzed the entire MkIV ground-based spectral dataset, consisting of 4200 spectra acquired on 1090 different days over the past 30 years.

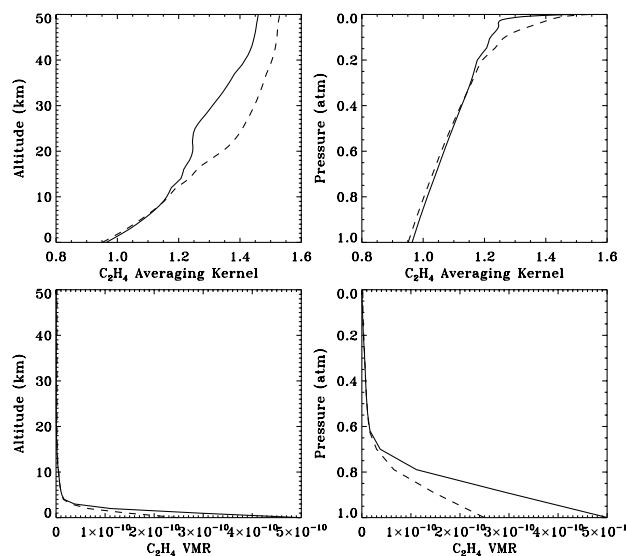


**Figure 3.** Averaging kernels (upper panels) and a priori profiles (lower panels) pertaining to the ground-based  $\text{C}_2\text{H}_4$  retrieval illustrated in Figs. 1 and 2. In the left panels quantities are plotted versus altitude. The right panels plot the same data versus atmospheric pressure. The solid line is the actual profile used. The dashed line is a vmr profile with a less dramatic decrease with altitude: the  $\text{C}_2\text{H}_4$  vmr below 4 km has been halved, with similar amounts in the upper troposphere, and more in the stratosphere. The resulting change in the retrieved total column is only 2%, with the dashed profile giving the lower columns.



125           The solid lines in Figure 3 shows the averaging kernel (upper panels) and a priori profile  
(lower panels) pertaining to the C<sub>2</sub>H<sub>4</sub> retrieval illustrated in Figures 1 and 2. The kernel  
represents the change in the total retrieved column due to the addition of one C<sub>2</sub>H<sub>4</sub> molecule.cm<sup>-2</sup>  
at a particular altitude. In a perfect column retrieval, the kernel would be 1.0 at all altitudes, but  
in reality the retrieval is more sensitive to C<sub>2</sub>H<sub>4</sub> at high altitudes than near the surface, as is  
130 typical for a profile-scaling retrieval of a weakly absorbing gas. The a priori vmr profile has a  
value of 500 ppt at the surface, dropping rapidly to 10 ppt by 5 km altitude. An even larger  
fractional drop, from 10 to 0.5 ppt occurs in the lower stratosphere between 15 and 21 km. The  
slight kink in the averaging kernel (solid line) over this same altitude range is due to this large  
drop in vmr. Since 99% of the C<sub>2</sub>H<sub>4</sub> lies in the troposphere, the stratospheric portion of the  
135 averaging kernel is of academic interest only for total column retrievals.

A major uncertainty in the retrieved column amounts is likely to be the smoothing error,  
which represents the effect of error in the a priori vmr profile. If the averaging kernel were  
perfect (i.e., 1.0 at all altitudes) this wouldn't matter, but in fact the C<sub>2</sub>H<sub>4</sub> kernels vary from 0.96  
at the ground to 1.4 at 40 km altitude. To investigate the sensitivity of the retrieved column to the  
140 assumed a priori profile, we also performed retrievals with a different a priori vmr profile in  
which the C<sub>2</sub>H<sub>4</sub> vmr profile had been halved in the 0-4 km altitude range and increased in the  
stratosphere, as depicted by the dashed line in Figure 3. The resulting change in the retrieved  
C<sub>2</sub>H<sub>4</sub> column was less than 2% with no discernable change to the rms fitting residuals, which are  
dominated by the interfering gases. This smallness of the C<sub>2</sub>H<sub>4</sub> column perturbation is a result of  
145 the averaging kernel being close to 1.0 at the altitudes with the largest a priori vmr errors (0 to 3  
km). Note that only errors in the *shape* of the a priori vmr profile affect the retrieved columns in  
a profile scaling retrieval.

Figure 4 shows the resulting MkIV ground-based C<sub>2</sub>H<sub>4</sub> columns from a dozen different  
observation sites. The plot is color-coded by the pressure altitude of the site. This was preferred  
150 over geometric altitude to prevent all the points from a given site piling up at exactly the same x-  
value. The pressure altitude varies by up to ±1.5% at the high altitude sites, which is equivalent  
to ±0.2 km. Only points with C<sub>2</sub>H<sub>4</sub> uncertainties <1x10<sup>15</sup> were included in the plot, representing  
95.7% of the total data volume. One day (out of 255) at Barcroft (3.8 km altitude) was omitted  
from the plotted data because it had abnormally high C<sub>2</sub>H<sub>4</sub>, as well as other short-lived gases --  
155 clearly a local pollution event.

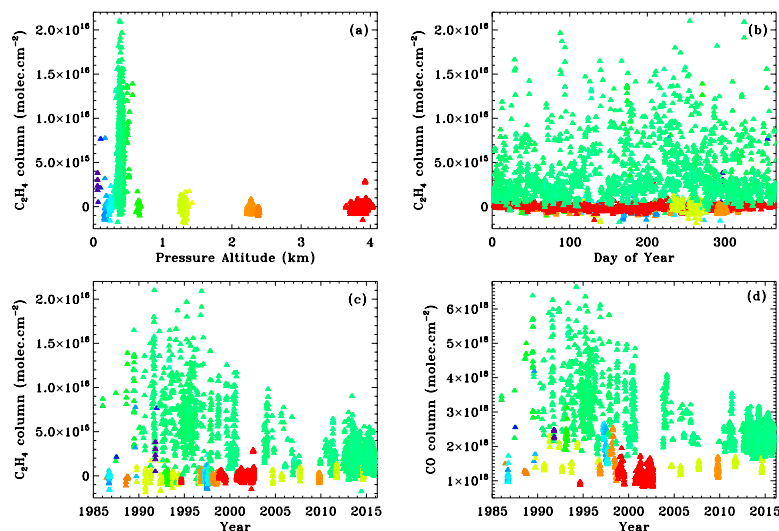


**Figure 4.** Retrieved MkIV column  $C_2H_4$  amounts from 12 different sites, color-coded by pressure altitude. Significant  $C_2H_4$  amounts are only found at the urban sites: JPL at 0.4 km altitude (green) and Mountain View at 0.05 km altitude (purple). Panel (b) reveals little seasonal variation in  $C_2H_4$ . Panel (c) shows a factor 3 decline in  $C_2H_4$  in Pasadena over the past 25 years. Panel (d) shows that the CO columns also decreased since 1990, but never come close to zero.

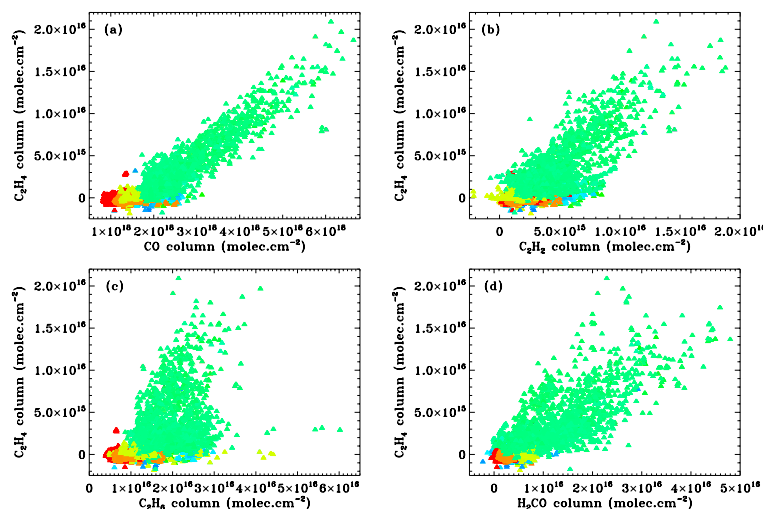
At all sites above 0.5 km altitude there is essentially no  $C_2H_4$ . The TMF site at 2.3 km altitude (orange) is only 25 km from the most polluted part of the Los Angeles basin, yet no measurable  $C_2H_4$  was recorded there in 45 observation days. This is probably a result of it always being above the PBL (Planetary Boundary Layer), in which urban pollution is trapped, at least on the autumn and winter days when MkIV made measurements at TMF. The high-latitude sites at Fairbanks, Esrange, and McMurdo also have no measurable  $C_2H_4$ , as do clean, rural, mid-latitude sites (e.g., Ft. Sumner, NM). The only sites where MkIV has ever detected  $C_2H_4$  are JPL/Pasadena (0.4 km; green) and Mountain View (0.01 km, purple). These sites are part of major conurbations: Pasadena adjoins Los Angeles; Mountain View adjoins San Jose, California.

At JPL the  $C_2H_4$  column is highly variable. JPL is located at the Northern edge of the Los Angeles conurbation, and so when winds are from the Northern sector, or strong from the ocean, pollution levels are much smaller than during stagnant conditions. This is seen in the large range of retrieved  $C_2H_4$  values observed at JPL throughout the year. A notable feature of the MkIV  $C_2H_4$  data (Fig. 4c) is the factor 3 drop over the past 25 years. Whereas in the 1990's  $C_2H_4$



often topped  $15 \times 10^{15}$  molec.cm<sup>-2</sup>, since 2010 a column exceeding  $7.5 \times 10^{15}$  has only been observed once.

180 Figure 4d shows the CO time series at JPL and Fig.5a shows its correlation with C<sub>2</sub>H<sub>4</sub>.  
The CO also shows a substantial decline since the 1990's at JPL, although not as dramatic as that  
of C<sub>2</sub>H<sub>4</sub> since CO never falls below  $1.5 \times 10^{18}$  molec.cm<sup>-2</sup> at JPL, even under the cleanest  
conditions. Figure 5a shows a tight correlation between C<sub>2</sub>H<sub>4</sub> and CO at JPL (green) suggesting a  
185 common local source for both. We believe this common source to be mainly vehicle exhaust and  
the declines in CO and C<sub>2</sub>H<sub>4</sub> to be a result of increasingly stringent requirements on vehicle  
emissions imposed by the US Environmental Protection Agency (EPA; e.g., the 1990 Clean Air  
Act) and the California Air Resources Board (CARB, LEV2) over the past decades and stronger  
enforcement thereof (e.g., smog checks).



190 **Figure 5.** Correlations between C<sub>2</sub>H<sub>4</sub> and four other gases: (a)=CO; (b)=C<sub>2</sub>H<sub>2</sub>, (c)=C<sub>2</sub>H<sub>6</sub>, and  
(d)=H<sub>2</sub>CO. The tightest correlation is with CO with a gradient of 0.0038 and a correlation  
coefficient of 0.93 for just the JPL-Pasadena data (green). Poorer correlations exist with the  
other gases. Points still color-coded by altitude, as in Figure 4.

195 Figure 5b/c/d also shows correlations between C<sub>2</sub>H<sub>4</sub> and other gases: C<sub>2</sub>H<sub>2</sub> and C<sub>2</sub>H<sub>6</sub>, and  
H<sub>2</sub>CO for all the MkIV measurements. These correlations are not as tight as that with CO, due to  
C<sub>2</sub>H<sub>2</sub> and C<sub>2</sub>H<sub>6</sub> have other sources. For example, C<sub>2</sub>H<sub>6</sub> also comes from natural gas leaks. The  
fact that these trace gases are much less abundant than CO means that their measurements are  
200 noisier, which also degrades the correlations.





Figure S1 plots the gas column relationship for the JPL ground-based data only, each panel containing ~1700 observations. The decreases in the CO, C<sub>2</sub>H<sub>2</sub>, C<sub>2</sub>H<sub>4</sub> and H<sub>2</sub>CO since the 1990's are evident by the lack of red points in the upper right of the panels plotting these gases.

205 C<sub>2</sub>H<sub>6</sub> seems not to have decreased significantly as is evident from the large values of the red points in the third row. In fact, on November 10, 2015, we observed a factor 2-3 enhancement of the C<sub>2</sub>H<sub>6</sub> column as a result of JPL being directly downwind of the Aliso Canyon natural gas leak on that day [Conley et al., 2916]. Although this event was associated with a 2.5% enhancements of column CH<sub>4</sub> (not shown here), there were no enhancements of CO, C<sub>2</sub>H<sub>2</sub>, C<sub>2</sub>H<sub>4</sub>, so these

210 particular C<sub>2</sub>H<sub>6</sub> points (red) in the third row of Fig. S1 protrude upwards from the main clusters.

Gas	CO (/ 1000)	C <sub>2</sub> H <sub>2</sub>	C <sub>2</sub> H <sub>4</sub>	C <sub>2</sub> H <sub>6</sub>
CO (/ 1000)				
215 C <sub>2</sub> H <sub>2</sub>	3.2±0.4 0.91			
C <sub>2</sub> H <sub>4</sub>	3.8±0.4 0.92	1.28±0.1 0.84		
C <sub>2</sub> H <sub>6</sub>	8.9±3.0 0.45	2.36±0.7 0.61	2.61±1.13 0.30	
H <sub>2</sub> CO	11.1±3.0 0.57	4.91±2.2 0.44	2.67±0.62 0.67	-10±14 -0.04

**Table 1.** Gradients of the fitted straight lines to the various panels in figure S1, together with their correlation coefficients. The gradients and their uncertainties are on the left of each cell, the CC values are italicized on the right. Note that the CO abundances have been divided by 1000 to bring them closer to the other gases. Thus the Gas:CO gradients are in units of ppt/ppb in the lower triangle, whereas the gradients of the non-CO gases are in ppt/ppt. In the second column, under the header "CO / 1000" the gradients could be termed "emission ratios".

220

225 The highest correlations are between CO and C<sub>2</sub>H<sub>2</sub> (0.91) and CO and C<sub>2</sub>H<sub>4</sub> (0.92). The correlation coefficient between C<sub>2</sub>H<sub>2</sub> and C<sub>2</sub>H<sub>4</sub> is only 0.84, probably reflecting the fact that C<sub>2</sub>H<sub>2</sub> and C<sub>2</sub>H<sub>4</sub> are much more difficult (i.e. noisier) measurements than CO. The worst correlation is between C<sub>2</sub>H<sub>6</sub> and H<sub>2</sub>CO (-0.04).

The overall gradient of the C<sub>2</sub>H<sub>4</sub>/CO relationship using all JPL data is 3.8±0.3 ppt/ppb, as

230 in Table 1, but the post-2010 data have a gradient of 2.7±0.4 ppt/ppb. Our overall value is lower than the 5.7 ppt/ppb measured by Baker et al. [2008] in Los Angeles from whole air canister samples acquired between 1999 and 2005, but close to their average of all US cities, 4.1 ppt/ppb. Warneke et al. [2007] report a C<sub>2</sub>H<sub>4</sub>/CO emissions ratio of 4.9 ppt/ppb in Los Angeles in 2002, measured by aircraft canister samples.



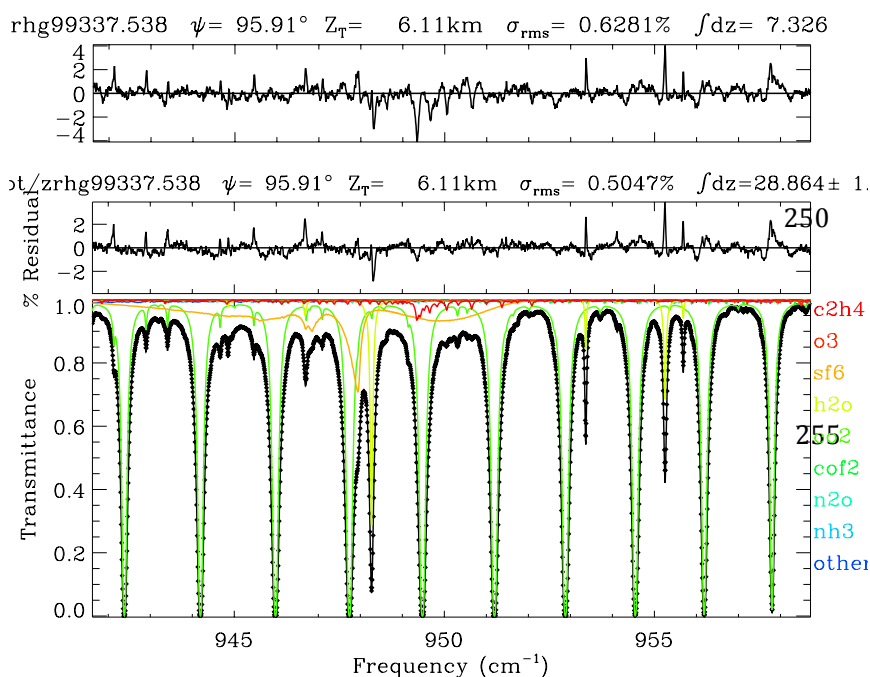
## 235 MkIV Balloon Results

We also looked for ethene in MkIV balloon spectra using exactly the same window, spectroscopy and fitting software (GFIT) as used for MkIV ground-based measurements. The advantage of the balloon spectra is that the airmass is much larger and the solar and instrumental features are removed from the occultation spectra by ratioing them against a high-sun spectrum taken at noon from float altitude.

240

Figure 6 shows a spectral fit to the MkIV balloon spectrum at 6 km tangent altitude measured above Esrange Sweden in Dec 1999. The peak  $C_2H_4$  absorption at  $949.35\text{ cm}^{-1}$  is about 6% deep, although this falls beneath a saturated  $CO_2$  lines. The information about  $C_2H_4$  at this and lower altitudes therefore comes from adjacent weaker features. At higher altitudes (not shown), where the  $CO_2$  lines are weaker and narrower, the  $C_2H_4$  information comes mainly from the  $949.35\text{ cm}^{-1}$  Q-branch.

245



260

**Figure 6.** Lower panel shows a fit to a MkIV balloon spectrum measured at 6 km tangent altitude. The  $C_2H_4$  absorption is denoted by the red line. Its Q-branch is seen at  $949.4\text{ cm}^{-1}$  reaching 6% in depth in this particular spectrum. In addition to  $C_2H_4$ , other gases were adjusted including  $O_3$ ,  $SF_6$ ,  $H_2O$ ,  $CO_2$ ,  $COF_2$ ,  $N_2O$ , and  $NH_3$ .  $CCl_2F_2$  and  $CH_3OH$  were included in the

265

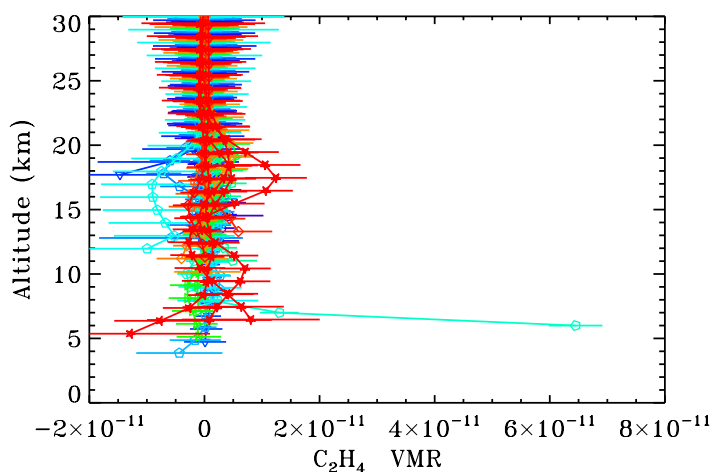


calculation but not adjusted. Middle panel shows residuals (measured minus calculated), which are mainly due to  $H_2O$ . Upper panel shows residuals after omitting  $C_2H_4$  from calculation, which increases the overall rms residual from 0.50% to 0.62%.

270 Figure 7 shows 30 balloon profiles of  $C_2H_4$  from 23 flights, color-coded according to date. Dark purple represents 1989, red represents 2014. The  $C_2H_4$  vmr retrieved from the Dec 1999 flight (green) was  $65 \pm 6$  ppt at 6 km, decreasing to  $14 \pm 4$  at 7 km, and undetectable above. The remaining balloon flights indicate a 10 ppt upper limit for  $C_2H_4$  in the free troposphere and 15 ppt in the stratosphere. Of course, these balloon flights were generally launched under calm, anti-cyclonic, clear-sky conditions, which tend to preclude transport of PBL pollutants up to the free troposphere. So there may be an inherent sampling bias in the MkIV balloon measurements that leads to low  $C_2H_4$ .

275 The balloon results are consistent with the ground-based measurements, confirming that  $C_2H_4$  exists in measurable quantities only in the polluted PBL, which is generally inaccessible by solar occultation due to the high aerosol content making the limb path opaque. The typical 1-3 day lifetime of  $C_2H_6$  at mid- and low-latitudes implies that it will only be measureable in the free troposphere soon after rapid uplift.

280



285 **Figure 7.** MkIV  $C_2H_4$  profiles from 24 balloon flights color-coded by year (purple = 1989; red = 2014). Altitude offsets of up to 0.4 km have been applied for clarity, to prevent the error bars from over-writing each other at each integer altitude. In only one flight, launched in Dec 1999 from Esrange, Sweden, was a significant amount of  $C_2H_4$  measured (green points at 6-7 km altitude). In other flights there was no detection, with upper limits varying from 10-15 ppt. The



290 *increase in uncertainty with altitude above 10 km is due to the C<sub>2</sub>H<sub>4</sub> absorption feature*  
*weakening in comparison with the spectral noise. Below 10 km the increasing uncertainty is due*  
*to the greater interference by H<sub>2</sub>O and CO<sub>2</sub>. Note that the negative C<sub>2</sub>H<sub>4</sub> values are all*  
*associated with large uncertainties.*

### Comparison with Remote Sensing Measurements

295 Paton-Walsh et al. [2005] measured up to  $300 \times 10^{15}$  molec.cm<sup>-2</sup> of C<sub>2</sub>H<sub>4</sub> during fire events  
in SE Australia in 2001-2003 with AODs of up to 5.5 at 500 nm wavelength (but not in MIR).  
Paton-Walsh et al. reported a tight relationship between AOD and biomass-burning products and  
established fire emission ratios.

From spectra acquired during one of the most intense of these fires (Jan 1, 2002),  
300 Rinsland et al. [2005] retrieved a total C<sub>2</sub>H<sub>4</sub> column of  $380 \pm 20 \times 10^{15}$  through a dense smoke  
plume and inferred a huge mole fraction of 37 ppb peaking at about 1 km above ground level.  
This retrieval used information from the shape of the Q-branch feature, which was nearly as deep  
as the overlapping CO<sub>2</sub> line. These C<sub>2</sub>H<sub>4</sub> amounts are 20 times larger than anything seen by  
MkIV, even from polluted JPL.

305 Coheur et al. [2007] reported a C<sub>2</sub>H<sub>4</sub> vmr of  $70 \pm 20$  ppt at 11.5 km altitude (their Table 2)  
in a biomass-burning plume, observed by the Atmospheric Chemistry Experiment (ACE)  
[Bernath et al., 2005] off the East coast of Africa. Their Fig. 2 shows measured C<sub>2</sub>H<sub>4</sub> exceeding  
100 ppt below 8 km. Simultaneous measurement of elevated C<sub>2</sub>H<sub>2</sub>, CO, C<sub>2</sub>H<sub>6</sub>, HCN and HNO<sub>3</sub>  
confirm their biomass-burning hypothesis.

310 Herbin et al. [2009] reported zonal-average ethene profiles above 6 km altitude based on  
global measurements by ACE. Figure 2 of et al. shows 35N zonal average vmrs of 40 ppt at 6  
km altitude, 30 ppt at 8 km, and 15 ppt at 14 km altitude, with error bars as small as 1 ppt. That  
said, Herbin et al. [2009] also wrote "We find that a value of 20 ppt is close to the detection  
threshold at all altitudes in the troposphere". Presumably, the 20 ppt detection limit refers to a  
315 single occultation whereas the 1 ppt error bar is the result of co-adding hundreds of ACE profiles.  
Herbin also report increasing C<sub>2</sub>H<sub>4</sub> with latitude. Although the ACE zonal means agree with the  
in situ measurements made during the PEM-West and TRACE-P, these campaigns were designed  
to measure the outflow of Asian pollution and therefore sampled some of the worst pollution on  
the planet. So one would expect lower values in a zonal average. Based on the total absence of  
320 negative values in any of their retrieved vmr profiles, we speculate that Herbin et al. [2009]  
performed a log(vmr) retrieval, imposing an implicit positivity constraint. This would have led  
to a noise-dependent, high bias in their retrieved profiles in places where C<sub>2</sub>H<sub>4</sub> was undetectable.



Clerbeaux et al. [2009] reported  $C_2H_4$  column abundances reaching  $3 \times 10^{15}$  molec. $cm^{-2}$  from spectra acquired by the IASI satellite instrument, a nadir-viewing emission sounder. This  
325 isolated event occurred on May 2008 over Eastern Asia and was associated with a Siberian fire  
plume, as confirmed by back-trajectories and co-located enhancements of  $CH_3OH$ ,  $HCOOH$  and  
 $NH_3$ .

More recently,  $C_2H_4$  was detected in boreal fire plumes (Alvarado et al., 2011; Dolan et  
al., 2016) during the 2008 ARCTAS mission by the Tropospheric Emission Sounder (TES), a  
330 nadir-viewing thermal emission FTS on board the Aura satellite. A strong correlation with CO  
was observed. TES's  $C_2H_4$  sensitivity depends strongly on the thermal contrast: the temperature of  
the  $C_2H_4$  relative to that of the underlying surface. For plumes in the free troposphere a detection  
limit of 2-3 ppb is claimed from a single sounding with a  $5 \times 8$  km footprint.

#### Comparison with In Situ Measurements

335 There are a lot of in situ ethane measurements. Here we intend to mention only those that  
are in some way comparable with MkIV measurements. These include measurements over the  
Western US. Profiles over the Pacific Ocean in the 30-40°N latitude range that are upwind of  
MkIV balloon measurements. Other measurements, e.g. over Europe and mainland SE Asia, are  
not relevant, given the 1-3 day lifetime of  $C_2H_4$ .

340 Gaffney et al. [2012] reported surface  $C_2H_4$  over Texas and neighboring states measured  
in 2002. They reported a median vmr of 112 ppt, with occasional much larger values of up to 2  
ppb, presumably when downwind of local sources. This median value, if present only within a  
150 mbar-thick PBL, represents a total column of  $0.3 \times 10^{15}$  molec. $cm^{-2}$ , which would be  
undetectable in ground-based MkIV measurements.

345 Lewis et al. [2013] reported airborne in situ measurements of non-methane organic  
compounds over SE Canada in summer 2010. The median ethane vmr was 49 ppt with plumes  
averaging 1848 ppt. Their  $C_2H_4/CO$  scatter plot (Fig. 2b of Lewis et al.) reveals two distinct  
branches. Biomass burning plumes show an emission ratio of 6.97ppt/ppb, whereas  
"local/anthropogenic emissions" show an emission ratio of about 1.3 ppt/ppb. These values  
350 bracket the MkIV value of  $3.7 \pm 0.5$  ppt/ppb obtained from the green points in Figs. 5a and all  
points of fig.S1 of the current paper.

Blake et al. [2003] report mean  $C_2H_4$  profiles from 0 to 12 km during the Feb-Apr 2001  
TRACE-P aircraft campaign, during which aircraft based in Hong Kong and Tokyo sampled  
outflow from SE Asia. Blake et al. compared these results with those from the similar 1991 and  
355 1994 PEM-West campaigns. Blake et al.'s Figure 11 shows that below 2 km  $C_2H_4$  averaged 100



ppt during TRACE P and 250 ppt during PEM-West. Blake et al.'s Table 1 provides a median  $C_2H_4$  of 30 ppt at 35N at 2-8 km altitude in the Western Pacific for both TRACE-P and PEM-West. Below 2 km the vmrs were much larger, especially during PEM-West. Blake et al.'s Figure 9 shows mean PBL vmrs of 200 ppt during Trace-P and 400 ppt during PEM-West, rapidly decreasing to 50 ppt by 4 km altitude, 30 ppt by 6 km, and less than 20 ppt above 9 km. Blake et al.'s Figure 2 shows high  $C_2H_4$  in the coastal margins of China, decreasing rapidly by a few hundred km off shore, consistent with the short  $C_2H_4$  lifetime. Since these aircraft campaigns were designed to measure polluted outflow from East Asia, their samples cannot be considered representative of a zonal average. Over the mid-Pacific,  $C_2H_4$  amounts were 0-15 ppt at all altitudes during TRACE-P and PEM-West B.

Sather and Cavender [2016] reported surface in situ measurements of ozone and Volatile Organic Compounds (including ethene) from the cities of Dallas-Ft. Worth, Houston, El Paso, Texas, and from Baton Rouge, Louisiana, over the past 30 years. For ethene the measurements, span the late 1990s to 2015, but nevertheless show clear declines by factors of 2-4 during 5-8am on weekdays. The authors attribute this decrease to the impacts of the 1990 amendment to the US Clean Air Act.

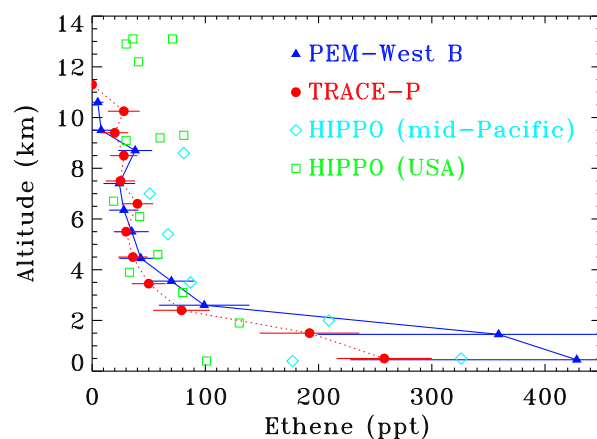


**Figure 8.** HIPPO in situ measurements of  $C_2H_4$  made by the Advanced Whole Air Sampler between  $30^\circ$  to  $40^\circ N$  are shown by cyan diamonds (mid-Pacific) and green squares (Central USA). PEM-West B (blue triangles) and TRACE-P (red circles) measurements of  $C_2H_4$  over coastal SE Asia and the Western Pacific (taken from Figure 9 of Blake et al. [2003]).

Ethene was measured during the HAIPER Pole-to-Pole (HIPPO; Wofsy et al. 2011, 2012) mission by the Advanced Whole Air Sampler. Figure 8 plots the  $C_2H_4$  vmrs measured in



380 the 30–40N latitude range. Points are color-coded by longitude. The blue points were measured  
mid-Pacific, red points over the Central/Western USA. Surprisingly,  $C_2H_4$  is larger over the mid-  
Pacific (blue/purple points) than the USA (red points) at altitudes below 9 km. This is  
presumably due to Asian pollution being further destroyed while crossing the Eastern Pacific.  
Above 9 km the  $C_2H_4$  is larger over the USA, presumably due to upward transport of the Asian  
385 pollution.

Washenfelder et al., [2011] performed ground-based in situ measurements from  
Pasadena, California, of several glyoxl pre-cursors in early June 2010, as part of the CalNEX  
2010 campaign. An ethene mole fraction of 2.16 ppb was reported. Assuming that this value was  
present throughout the PBL, extending from the surface at 1000 mbar to the 900 mbar level, then  
390 the in situ measurement implies a total  $C_2H_4$  column of  $4 \times 10^{15}$  molec. $cm^{-2}$ , which is consistent  
with the upper range of values observed by MkIV in 2010. Unfortunately we do not have  
overlapping measurements, and in any case JPL is 10 km from the Caltech site used by  
Washenfelder et al. [2011].

Washenfelder et al., [2011] also report a factor 6 drop in  $C_2H_4$  amounts since the  
395 September 1993 CalNEX campaign, but note that the 1993 readings occurred during a smog  
episode, implying higher than normal levels of pollution. This drop is larger than the factor 3  
decrease seen in the MkIV column data, but not inconsistent given the sparse statistics together  
with the large day-to-day variability seen in the MkIV data.

Measurements of ethene in Mexico City ranged between 10–60 ppb, with higher levels in  
400 the commercial sectors and lower values in residential areas (Altuzar et al., 2001, 2005; Velasco  
et al., 2007). These are 5–30 times larger than the 2.16 ppb measured by Washenfelder et al.  
[2011] in Pasadena in 2010.

## Discussion

To see whether the ground-based MkIV  $C_2H_4$  measured in Pasadena was correlated with  
405 the air mass origin, we performed HYSPLIT back-trajectories, and computed the amount of time  
that air masses arriving 500 m above JPL had spent over the highly populated areas of Los  
Angeles conurbation. When column  $C_2H_4$  was plotted versus this time-over-conurbation, the  
correlation was very poor. Column CO also had a poor correlation. The fact that the  $C_2H_4$   
correlates well with CO tends to discount the possibility that the  $C_2H_4$  measurements are wrong,  
410 since the CO measurements are very reliable. So this implies that either the trajectories are  
wrong, or that the urban pollution is not a major source of the  $C_2H_4$  or CO observed by MkIV.  
We point out that JPL is located at the foot of the San Gabriel mountains, which rise over 1 km



above JPL over a horizontal distance of less than 5 km. This extreme topography might give rise to complexities in the wind fields that might be inadequately represented in the EDAS 40 km-  
415 resolution model. Although higher resolution models (e.g. NAM 12km) are available for doing HYSPLIT trajectories, these cover only the past decade, whereas the JPL MkIV measurements go back more than 30 years.

$C_2H_4/CO$  emission ratios measured over Pasadena by MkIV have decreased over the 30 year record, from  $3.8 \pm 0.5$  ppt/ppb overall to  $2.8 \pm 0.4$  ppt/ppb in recent years. It is not clear what  
420 is causing this decrease since many things have changed that might affect  $C_2H_4$  levels (e.g. regulation of internal combustion engine exhaust, elimination of oil-based paints and lighter fuel, better control of emissions from oil and gas wells). One possibility is decreasing pollution from biomass burning, which causes higher  $C_2H_4/CO$  emission ratios [Lewis et al., 2013].

### Summary and Conclusions

425 A 30-year record of atmospheric  $C_2H_4$  has been extracted from ground-based FTIR spectra measured by the JPL MkIV instrument. Despite its high sensitivity, MkIV only detects ethene at polluted urban sites (e.g., Pasadena, California). At clean sites visited by MkIV,  $C_2H_4$  was undetectable (less than  $10^{15}$  molec. $cm^{-2}$ ). MkIV ground-based measurements are generally consistent with the available surface in situ measurements, although a definitive comparison is  
430 difficult due to the large variability of  $C_2H_4$  and lack of co-incidence.

A large decline in  $C_2H_4$  has been observed over Pasadena over the past 25 years. This is likely the a result of increasingly stringent requirements on vehicle emissions imposed by the US Environmental Protection Agency (e.g., the 1990 Clean Air Act) and the California Air Resources Board (Low Emission Vehicle 2 requirements) over the past decades, together with stronger  
435 enforcement of these regulations (e.g., smog checks). The  $C_2H_4/CO$  emissions ratio also appears to have decreased in recent years.

This work shows that  $C_2H_4$  might in future become a routine product of the NDACC Infra-Red FTS network, at least at sites with local sources. Moreover, since the spectra are saved, a historical  $C_2H_4$  record may be retro-actively extractable at some of the more polluted sites.

440 MkIV balloon measurements have only detected ethane once in 24 flights: in the Arctic in December 1999 at altitudes below 6 km. In all other flights an upper limit of 15 ppt was established for the free troposphere and 10 ppt for the lower stratosphere. These upper limits are substantially smaller than the ACE 35N zonal mean profiles reported by Herbin et al. [2009], which are possibly biased high when  $C_2H_4$  amounts are small due to a positivity constraint  
445 imposed on the retrievals. Also, a single biomass burning plume with up to 25 ppb of  $C_2H_4$  has





the potential to significantly increase the zonal mean C<sub>2</sub>H<sub>4</sub>. For this reason, a zonal median would be a more robust statistic. It is also possible that the MkIV balloon flights under-represent conditions in which PBL pollution is lofted due to their location and the meteorology associated with balloon launches. Herbin et al. [2009] reported an increase of the 6-km ACE C<sub>2</sub>H<sub>4</sub> with  
450 latitude in the Northern hemisphere, peaking at 53 ppt at 70N. This is consistent with the December 1999 MkIV balloon flight from 67N, which measured 60 ppt at 6 km.

MkIV balloon measurements over the Western USA are much lower than in situ aircraft measurements over SE Asia during TRACE-P, PEM-West B, and over the mid-Pacific ocean during HIPPO. With its 1-3 day lifetime, C<sub>2</sub>H<sub>4</sub> decreases substantially during its Eastward  
455 journey across the Pacific, which would help reconcile them with the MkIV balloon profiles.

**Acknowledgements.** This research was performed at the Jet Propulsion Laboratory, California Institute of Technology, under contract with NASA. We thank the Columbia Scientific Balloon Facility (CSBF) who conducted the majority of the balloon flights. We thank the CNES Balloon  
460 Launch facility who conducted four MkIV balloon flights from Esrange, Sweden. We thank the Swedish Space Corporation for their support and our use of their facilities. Finally, we acknowledge support from the NASA Upper Atmosphere Research Program.

## References

- Altuzar, V., Pacheco, M., Tomas, S.A., Arriaga, J.L., Zelaya-Angel, O., SanchezSinencio, F.,  
465 2001. Analysis of ethylene concentration in the Mexico City atmosphere by photoacoustic spectroscopy. *Analytical Sciences* 17, 541-543.
- Altuzar, V., Tomás, S.A., Zelaya-Angel, O., Sánchez-Sinencio, F., Arriaga, J.L., 2005. Atmospheric ethene concentrations in Mexico City: indications of strong diurnal and seasonal dependences. *Atmospheric Environment* 39, 5215-5225.
- 470 Alvarado, M.J., Cady-Pereria, K.E., Xiao, Y., Millet, D.B., Payne, V.H., 2011. Emission ratios for ammonia and formic acid and observations of peroxy acetyl nitrate (PAN) and ethylene in biomass burning smoke as seen by the tropospheric emission spectrometer (TES). *Atmosphere*, 2, 633-644. <http://dx.doi.org/10.3390/atmos2040633>.
- 475 Baker, A. K.; Beyersdorf, A. J.; Doezema, L. A.; Katzenstein, A.; Meinardi, S.; Simpson, I. J.; Blake, D. R.; Rowland, F. S., Measurements of nonmethane hydrocarbons in 28 United States cities. *Atmos. Environ.* 2008, 42, 170-182.



- Bernath, P.F., McElroy, C.T., Abrams, M.C., Boone, C.D., Butler, M., Camy-Peyret, C., Carleer, M., Clerbaux, C., Coheur, P.F., Colin, R. and DeCola, P., 2005. Atmospheric chemistry experiment (ACE): mission overview. *Geophysical Research Letters*, 32(15).
- 480 Blake, N. J., et al. (2003), NMHCs and halocarbons in Asian continental outflow during the Transport and Chemical Evolution over the Pacific (TRACE-P) field campaign: Comparison with PEM-West B, *J. Geophys. Res.*, 108(D20), 8806, doi:10.1029/2002JD003367.
- Clerbaux, C., Boynard, A., Clarisse, L., George, M., Hadji-Lazaro, J., Herbin, H., Hurtmans, D., Pommier, M., Razavi, A., Turquety, S., Wespes, C., and Coheur, P.-F.: Monitoring of  
485 atmospheric composition using the thermal infrared IASI/MetOp sounder, *Atmos. Chem. Phys.*, 9, 6041-6054, doi:10.5194/acp-9-6041-2009, 2009.
- Coheur, P-F., et al. "ACE-FTS observation of a young biomass burning plume: first reported measurements of C<sub>2</sub>H<sub>4</sub>, C<sub>3</sub>H<sub>6</sub>O, H<sub>2</sub>CO and PAN by infrared occultation from space." *Atmospheric chemistry and physics* 7.20 (2007): 5437-5446
- 490 Conley, S., G. Franco, I. Faloon, D. R. Blake, J. Peischl, T. B. Ryerson, Methane emissions from the 2015 Aliso Canyon blowout in Los Angeles, CA, *Science*, 2016, DOI: 10.1126/science.aaf2348
- Dolan, Payne, Kualwik, and Bowman, Satellite observations of ethylene (C<sub>2</sub>H<sub>4</sub>) from the Aura Tropospheric Emission Spectrometer: A scoping study, *Atmospheric Environment*, 141,  
495 (2016), 388–393
- Gaffney, Jeffrey S., Nancy A. Marley, Donald R. Blake, Baseline measurements of ethene in 2002: Implications for increased ethanol use and biomass burning on air quality and ecosystems, *Atmospheric Environment* 56 (2012), 161-168
- Herbin, H., Hurtmans D., Clarisse L., Turquety S., Clerbaux C., Rinsland C. P., Boone C.,  
500 Bernath P. F., and Coheur P.- F.: Distributions and seasonal variations of tropospheric ethene (C<sub>2</sub>H<sub>4</sub>) from Atmospheric Chemistry Experiment (ACE-FTS) solar occultation spectra, *Geophys. Res. Lett.*, 36, L04801, doi:10.1029/2008GL036338, 2009.
- Hough A.M. (1991). Development of a two-dimensional global troposphere model: Model chemistry. *J. Geophys. Res.*, 96, 7325-7362.
- 505 Lewis, A. C., M. J. Evans, J. R. Hopkins, S. Punjabi, K. A. Read, R. M. Purvis, S. J. Andrews, S. J. Moller, L. J. Carpenter, J. D. Lee, A. R. Rickard, P. I. Palmer, and M. Parrington, The influence of biomass burning on the global distribution of selected non-methane organic compounds, *Atmos. Chem. Phys.*, 13, 851–867, 2013, doi:10.5194/acp-13-851-2013



- Müller, Jean-François, and Guy Brasseur. "IMAGES: A three-dimensional chemical transport  
510 model of the global troposphere." *Journal of Geophysical Research: Atmospheres* 100.D8  
(1995): 16445-16490.
- Olivella, Santiago, and Albert Solé. "Unimolecular decomposition of  $\beta$ -hydroxyethylperoxy  
radicals in the HO-initiated oxidation of ethene: A theoretical study." *The Journal of Physical  
Chemistry A* 108.52 (2004): 11651-11663.
- 515 Paton-Walsh, C., N. B. Jones, S. R. Wilson, V. Haverd, A. Meier, D. W. T. Griffith, and C. P.  
Rinsland (2005), Measurements of trace gas emissions from Australian forest fires and  
correlations with coincident measurements of aerosol optical depth, *J. Geophys. Res.*, 110,  
D24305, doi:[10.1029/2005JD006202](https://doi.org/10.1029/2005JD006202).
- Irion, F.W., M.R. Gunson, G.C. Toon, A.Y. Chang, A. Eldering, E. Mahieu, G.L. Manney, H.A.  
520 Michelsen, E.J. Moyer, M.J. Newchurch, G.B. Osterman, C.P. Rinsland, R.J. Salawitch, B.  
Sen, Y.L. Yung, and R. Zander, Atmospheric Trace Molecule Spectroscopy (ATMOS)  
Experiment Version 3 data retrievals, *Appl. Opt.*, 41(33), 6968-6979, 2002.
- Rothman, L. S., Gordon, I. E., Babikov, Y., Barbe, A., Chris Benner, D., Bernath, P. F., Birk, M.,  
Bizzocchi, L., Boudon, V., Brown, L. R., Campargue, A., Chance, K., Cohen, E. A., Coudert,  
525 L. H., Devi, V. M., Drouin, B. J., Fayt, A., Flaud, J.-M., Gamache, R. R., Harrison, J. J.,  
Hartmann, J.-M., Hill, C., Hodges, J. T., Jacquemart, D., Jolly, A., Lamouroux, J., Le Roy, R.  
J., Li, G., Long, D. A., Lyulin, O. M., Mackie, C. J., Massie, S. T., Mikhailenko, S., Müller,  
H. S. P., Naumenko, O. V., Nikitin, A. V., Orphal, J., Perevalov, V., Perrin, A., Polovtseva,  
E. R., Richard, C., Smith, M. A. H., Starikova, E., Sung, K., Tashkun, S., Tennyson, J., Toon,  
530 G. C., Tyuterev, V. I. G., and Wagner, G.: The HITRAN2012 Molecular Spectroscopic  
Database, *J. Quant. Spectrosc. Ra.*, 130, 4–50, 2013.
- Rothman, L.S., A. Barbe, D. Chris Benner, L.R. Brown, C. Camy-Peyret, M.R. Carleer, K.  
Chance, C. Clerbaux, V. Dana, V.M. Devi, A. Fayt, J.-M. Flaud, R.R. Gamache, A.  
Goldman, D. Jacquemart, K.W. Jucks, W.J. Lafferty, J.-Y. Mandin, S.T. Massie, V.  
535 Nemtchinov, D.A. Newnham, A. Perrin, C.P. Rinsland, J. Schroeder, K.M. Smith, M.A.H.  
Smith, K. Tang, R.A. Toth, J. Vander Auwera, P. Varanasi, K. Yoshino, The HITRAN  
molecular spectroscopic database: edition of 2000 including updates through 2001, *Journal  
of Quantitative Spectroscopy & Radiative Transfer* 82 (2003) 5–44
- Rinsland, C., Paton-Walsh, C., Jones, N. B., Griffith, D. W., Goldman, A., Wood, S., Chiou, L. &  
540 Meier, A. (2005). High Spectral resolution solar absorption measurements of ethylene ( $C_2H_4$ )  
in a forest fire smoke plume using HITRAN parameters: Tropospheric vertical profile  
retrieval. *Journal of Quantitative Spectroscopy and Radiative Transfer*, 96 (2), 301-309.



- Sather, M.E., K, Cavender. Trends analyses of 30 years of ambient 8 hour ozone and precursor monitoring data in the South Central U.S.: progress and challenges, *Environ. Sci.: Processes Impacts*, 2016, **18**, 819-831
- 545
- Sawada S., Totsuka T. Natural and anthropogenic sources and fate of atmospheric ethylene. *Atmospheric environment*, 20, 821-832, DOI: 10.1016/0004-6981(86)90266-0, 1986
- Sen, B., G.C. Toon, J.-F. Blavier, E.L. Fleming, and C.H. Jackman, Balloon-borne observations of mid-latitude fluorine abundance, *J. Geophys. Res.*, 101(D4), 9045-9054, 1996.
- 550
- Toon, G.C., The JPL MkIV Interferometer, *Opt. Photonics News*, 2, 19-21, 1991.
- Toon, G. C., J.-F. Blavier, B. Sen, R. J. Salawitch, G. B. Osterman, J. Notholt, M. Rex, C. T. McElroy, and J. M. Russell III (1999a), Ground-based observations of Arctic O<sub>3</sub> loss during spring and summer 1997, *J. Geophys. Res.*, 104 (D21), 26497–26510, doi:10.1029/1999JD900745.
- 555
- Toon, G.C., J.-F. Blavier, B. Sen, J.J. Margitan, C.R. Webster, R.D. May, D.W. Fahey, R. Gao, L. Del Negro, M. Proffitt, J. Elkins, P.A. Romashkin, D.F. Hurst, S. Oltmans, E. Atlas, S. Schauffler, F. Flocke, T.P. Bui, R.M. Stimpfle, G.P. Bonne, P.B. Voss, and R.C. Cohen, Comparison of MkIV balloon and ER-2 aircraft profiles of atmospheric trace gases, *J. Geophys. Res.*, 104, 26,779-26,790, 1999b.
- 560
- Toon, G. C. 2014a. Telluric line list for GGG2014. TCCON data archive, hosted by the Carbon Dioxide Information Analysis Center, Oak Ridge National Laboratory, U.S.A. <http://dx.doi.org/10.14291/tcon.ggg2014.atm.R0/1221656>
- Toon, G. C. 2014b. Solar line list for GGG2014. TCCON data archive, hosted by the Carbon Dioxide Information Analysis Center, Oak Ridge National Laboratory, U.S.A. <http://dx.doi.org/10.14291/tcon.ggg2014.atm.R0/1221658>
- 565
- Toon, G.C., J.-F. Blavier, K. Sung, L.S. Rothman, I. Gordon, HITRAN spectroscopy evaluation using solar occultation FTIR spectra, *J. Quant. Spectrosc. Radiat. Transfer* (2016), <http://dx.doi.org/10.1016/j.jqsrt.2016.05.21>
- Velasco, E., Lamb, B., Westberg, H., Allwine, E., Sosa, G., Arriaga-Colina, J.L., Jobson, B.T., Alexander, M., Prazeller, P., Knighton, W.B., Rogers, T.M., Grutter, M., Herndon, S.C., Kolb, C.E., Zavala, M., de Foy, B., Volkamer, R., Molina, L.T., Molina, M.J., 2007. Distribution, magnitudes, reactivities, ratios and diurnal patterns of volatile organic compounds in the Valley of Mexico during the MCMA 2002 and 2003 field campaigns. *Atmospheric Chemistry and Physics* 7, 329-353.
- 575
- Wunch, D., G. C. Toon, J.-F. L. Blavier, R. A. Washenfelder, J. Notholt, B. J. Connor, D. W. T. Griffith, V. Sherlock, and P. O. Wennberg (2011), The total carbon column observing



- network, *Philosophical Transactions of the Royal Society - Series A: Mathematical, Physical and Engineering Sciences*, 369(1943), 2087-2112, doi:10.1098/rsta.2010.0240.
- 580 Washenfelder, R. A., et al. (2011), The glyoxal budget and its contribution to organic aerosol for Los Angeles, California, during CalNex 2010, *J. Geophys. Res.*, 116, D00V02, doi:[10.1029/2011JD016314](https://doi.org/10.1029/2011JD016314).
- 585 Warneke, C.; McKeen, S. A.; De Gouw, J. A.; Goldan, P. D.; Kuster, W. C.; Holloway, J. S.; Williams, E. J.; Lerner, B.; Parrish, D. D.; Trainer, M.; Fehsenfeld, F. C.; Kato, S.; Atlas, E. L.; Baker, A.; Blake, D. R., Determination of urban volatile organic compound emission ratios and comparison with an emissions database. *J. Geophys. Res.-Atmos.* 2007, 112, D10S47.
- 590 Wofsy, S. C., THE HIPPO SCIENCE TEAM AND COOPERATING MODELLERS AND SATELLITE TEAMS, HIAPER Pole-to-Pole Observations (HIPPO): fine-grained, global-scale measurements of climatically important atmospheric gases and aerosols, *Phil. Trans. R. Soc. A* (2011) 369, 2073–2086 doi:10.1098/rsta.2010.0313
- 595 Wofsy, S. C., B. C. Daube, R. Jimenez, E. Kort, J. V. Pittman, S. Park, R. Commane, B. Xiang, G. Santoni, D. Jacob, J. Fisher, C. Pickett-Heaps, H. Wang, K. Wecht, Q.-Q. Wang, B. B. Stephens, S. Shertz, A.S. Watt, P. Romashkin, T. Campos, J. Haggerty, W. A. Cooper, D. Rogers, S. Beaton, R. Hendershot, J. W. Elkins, D. W. Fahey, R. S. Gao, F. Moore, S. A. Montzka, J. P. Schwarz, A. E. Perring, D. Hurst, B. R. Miller, C. Sweeney, S. Oltmans, D. Nance, E. Hints, G. Dutton, L. A. Watts, J. R. Spackman, K. H. Rosenlof, E. A. Ray, B. Hall, M. A. Zondlo, M. Diao, R. Keeling, J. Bent, E. L. Atlas, R. Lueb, M. J. Mahoney. 2012. HIPPO Merged 10-second Meteorology, Atmospheric Chemistry, Aerosol Data (R\_20121129). Carbon Dioxide Information Analysis Center, Oak Ridge National Laboratory, Oak Ridge, Tennessee, U.S.A. [http://dx.doi.org/10.3334/CDIAC/hippo\\_010](http://dx.doi.org/10.3334/CDIAC/hippo_010) (Release 20121129)
- 600
- 605 Xue, Likun, Tao Wang, Isobel. J. Simpson, Aijun Ding , Jian Gao , Donald. R. Blake , Xuezhong Wang , Wenxing Wanga, Hengchi Lei, Dezhen Jin, Vertical distributions of non-methane hydrocarbons and halocarbons in the lower troposphere over northeast China, *Atmospheric Environment* 45, (2011), 6501-6509